Multi-Access Interference Suppression in Canonical Space–Time Coordinates: A Decentralized Approach

Eko N. Onggosanusi, *Member, IEEE*, Akbar M. Sayeed, *Member, IEEE*, and Barry D. Van Veen, *Fellow, IEEE*

***Abstract*—We propose a decentralized space–time multiuser detection scheme based on the notion of canonical space–time coordinates (CSTCs) for representing the received signal. The CSTC representation provides a natural framework for decentralized multi-access interference (MAI) suppression in lower dimensional subspaces that results in complexity reduction relative to existing chip rate filtering schemes. The framework is based on a partitioning of the signal space into active and inactive CSTCs. The active CSTCs contain the signal of the desired user, facilitate maximal diversity exploitation and minimal complexity interference suppression. The inactive CSTCs only contain MAI and can be included progressively to attain a desired level of MAI suppression at the cost of increased complexity. We develop CSTC-based linear coherent multiuser detectors using the linearly constrained minimum variance (LCMV) criterion. We characterize the set of inactive coordinates and analyze the performance of the LCMV receiver as a function of the number of inactive CSTCs. Channel estimation and detector sensitivity to channel estimation errors are discussed. We demonstrate that the low-complexity adaptive receivers designed via the CSTC framework are more robust to channel estimation errors than existing chip-domain filtering schemes.**

***Index Terms*—Antenna arrays, interference suppression, multipath, multiuser detectors, space–time signal processing.**

I. Introduction

CODE–DIVISION multiple–access (CDMA) systems have emerged as a prominent wireless technology as evident from their prevalence in emerging standards. Multi-access interference (MAI) is one of the most important factors that limits the performance of CDMA systems. Recent interest in antenna array and space–time processing techniques has been motivated by the need to suppress MAI. There has been considerable recent research into decentralized MAI suppression techniques that only require knowledge of the spreading code of the desired user and are thus applicable to mobile handsets. Most existing techniques are based on chip-domain filtering (see, e.g., [1]–[5]) that employ receiver processing in the full-dimensional signal space.

There are two main drawbacks of existing techniques based on chip-domain filtering. First, most techniques do not account for multipath effects in a satisfactory fashion—multipath dispersion is often treated as uncertainty in the knowledge of the desired user's signature waveform (see, e.g., [2]). Second, many existing techniques either ignore the issue of complexity or propose *ad hoc* methods for complexity reduction. For example, multipath dispersion effects are addressed in an elegant fashion in [6] but the proposed receivers operate in the full-dimensional signal space thereby offering no mechanism for complexity reduction. Dimensionality reduction is critical in decentralized receivers since they often have limited computational capability and need rapid and reliable estimates of required statistics. Indeed, full-dimensional receivers based on chip-domain filtering suffer significant degradation in performance in mobile scenarios due to errors in estimation of required statistics (see, for example, [7]). Some rank reduction techniques have been recently proposed to reduce complexity (see, e.g., [8]–[11]). However, these techniques generally require additional computation and data to determine the subspace used for adaptation. Further complexity reduction is possible when the interference suppression in spatial and temporal domains is separated. Examples of such schemes can be found in [12]–[15]. However, such separation may lead to significant performance loss.

In this paper, we introduce a framework for decentralized multiuser detection based on notion of canonical space–time coordinates (CSTCs) [16]. The CSTC representation provides a parsimonious characterization of the received signal in terms of *fixed* basis signals corresponding to certain *discrete* multipath delays and directions-of-arrival (DOAs) of the signaling waveform. The use of fixed basis functions inherently eliminates the need for estimating arbitrary delays and DOAs. As we demonstrate in this paper, the CSTC framework fully accounts for multipath propagation effects and provides a systematic framework for controlling receiver complexity to attain a desired level of MAI suppression. Compared to the existing chip-domain filtering approaches, significant complexity reduction can be obtained, especially in channels with dense multipath and relatively small delay and angular spread. Such channels often occur in practice for wide-band communication scenarios. While the focus of this paper is on decentralized receivers, the CSTC framework can be leveraged in centralized scenarios as well [17].

At the heart of our MAI suppression framework is a partitioning of the signal space into active and inactive CSTCs. The desired user's signal is concentrated in the active coordinates that depend on its delay and angle spreads. The inactive coordinates are outside the channel spread of the user and do not contain the desired signal. MAI generally occupies both active and inactive coordinates. We develop CSTC-based de-

Paper approved by S. L. Miller, the Editor for Spread Spectrum of the IEEE Communications Society. Manuscript received March 27, 2000; revised January 3, 2001, and October 16, 2001. This work was supported in part by the National Science Foundation under Awards ECS-9979448 and CCR-9875805.

E. N. Onggosanusi is with the DSPS & R&D Center, Texas Instruments Incorporated, Dallas, TX 75243 USA.

A. M. Sayeed and B. D. Van Veen are with the Department of Electrical and Computer Engineering, University of Wisconsin-Madison, Madison, WI 53706 USA (e-mail: vanveen@engr.wisc.edu).

Publisher Item Identifier S 0090-6778(02)05107-3.

centralized space–time multiuser detectors using the linearly constrained minimum variance (LCMV) criterion [18], which facilitates adaptive receiver implementation. While the active CSTCs capture the essential diversity and energy of the desired user's signal, they only provide limited MAI suppression. Progressively improved MAI suppression can be attained at the cost of increased complexity by using a subset of inactive coordinates in conjunction with active coordinates. We note that the notion of active and inactive coordinates is implicitly used in the decentralized detectors based on aperiodic spreading codes proposed in [19] and [20]. However, our focus is on systems employing periodic codes.

CSTC-based multiuser detectors are also advantageous from the viewpoint of adaptive implementation. First, the number of CSTC channel parameters that need to be estimated is smaller than that in existing chip-domain filtering approaches, especially for limited multipath and angular spreads. Furthermore, the systematic control of the degrees of freedom (active and inactive coordinates) in the receiver afforded by the CSTC framework facilitates accurate estimation of statistics required in adaptive receivers, particularly in fast fading scenarios. Finally, the CSTC framework also suggests a serial MAI suppression scheme, not possible in chip-domain filtering schemes, which greatly reduces the receiver sensitivity to channel estimation errors.

The rest of this paper is organized as follows. Section II describes the multiuser CSTC representation. Section III discusses the design of LCMV-based decentralized detectors, followed by performance analysis in Section IV. Extension to general binary signaling and noncoherent detection is given in Section V. Section VI discusses blind channel estimation and sensitivity to channel estimation errors. A concrete comparison between CSTC-based receivers and chip-domain filtering schemes in Section VII highlights the advantages of the proposed framework. Examples are given in Section VIII, followed by conclusions in Section IX.

The following notation is used throughout the paper. Superscript T and H indicate matrix transpose and conjugate transpose, respectively. Uppercase boldface letters denote matrices while lowercase boldface letters indicate column vectors. $\mathbf{I}_N$ denotes the $N \times N$ identity matrix. A complex circular Gaussian vector $\mathbf{x}$ with mean $\mathbf{m}$ and covariance matrix $\mathbf{R}$ is denoted as $\mathbf{x} \sim \mathcal{N}_C[\mathbf{m}, \mathbf{R}]$. The statistical expectation operator is written as $\mathrm{E}[.]$ and Euclidean norm of vector $\mathbf{x}$ is denoted as $\|\mathbf{x}\|$.

II. CSTC Representation for Multiuser Systems

Consider a frequency-selective, slow fading channel with K users. The baseband signal $\mathbf{r}(t) \in \mathbb{C}^R$ received at an R-element array within one symbol duration T can be written as

$$\mathbf{r}(t) = \sum_{k=1}^{K} b_k \sqrt{\rho_k}\, \mathbf{s}_k(t - \tau_k) + \mathbf{n}(t) \tag{1}$$

$$\mathbf{s}_k(t) = \int_{S_k^-}^{S_k^+} \int_0^{T_k} H_k(\phi, \tau)\, \mathbf{a}(\phi)\, q_k(t - \tau)\, d\tau\, d\phi \tag{2}$$

where b_k, ρ_k and τ_k are the symbol, power, and delay of the kth user. Here, $\mathbf{a}(\phi)$ is the array response vector for DOA ϕ, and $H_k(\phi, \tau)$ is the angle-dependent impulse response of the channel. The symbols $q_k(t)$, $[S_k^-, S_k^+]$, and $[0, T_k]$ denote the signaling waveform, angular spread, and delay spread for the kth user, respectively. We initially assume binary antipodal signaling with $b_k \in \{\pm 1\}$. The vector $\mathbf{n}(t)$ is zero-mean complex Gaussian noise with $E[\mathbf{n}(t)\mathbf{n}^H(t')] = \sigma^2 \mathbf{I}_R \delta(t - t')$ and is independent of $\{b_k\}$.

Due to the essentially band-limited nature of $q_k(t)$, the kth user signal admits a representation [16]

$$\mathbf{s}_k(t - \tau_k) \approx \sum_{p=P_k^-}^{P_k^+} \sum_{l=d_k}^{d_k + L_k} H_{k,pl}\, \mathbf{q}_{k,pl}(t) \tag{3}$$

$$\mathbf{q}_{k,pl}(t) = \mathbf{a}(\varphi_p) q_k\left(t - \frac{l}{B}\right), \qquad 0 \le t < T \tag{4}$$

where B is the effective (two-sided) bandwidth and the R *fixed* angles, $\varphi_1 < \varphi_2 < \cdots < \varphi_R$, are chosen such that $\{\mathbf{a}(\varphi_p)\}_{p=1}^R$ are linearly independent. The number of terms in (3) represents the level of spatio–temporal diversity provided by the channel and is determined by $d_k = \lfloor \tau_k B \rfloor$, $L_k = \lceil T_k B \rceil$, $P_k^+ = \min_i\{\varphi_i \ge S_k^+\}$, $P_k^- = \max_i\{\varphi_i \le S_k^-\}$. Without loss of generality, $q_k(t)$ and $\mathbf{a}(\phi)$ are chosen as unit-energy. *User 1* is assumed to be the desired user with $\rho_1 = 1$ and $\tau_1 = 0$; that is, perfect timing acquisition is assumed for the desired user.

Define the array response matrix and temporal basis vector, respectively, as

$$\mathbf{A}_k \stackrel{\text{def}}{=} \left[\mathbf{a}\left(\varphi_{P_k^-}\right), \ldots, \mathbf{a}\left(\varphi_{P_k^+}\right)\right] \tag{5}$$

$$\boldsymbol{\psi}_k(t) \stackrel{\text{def}}{=} \left[q_k\left(t - \frac{d_k}{B}\right), \ldots, q_k\left(t - \frac{d_k + L_k}{B}\right)\right]^T \tag{6}$$

and let $\mathbf{H}_k$ be the channel coefficient matrix with (p, l) element $H_{k,pl}$. The received signal $\mathbf{r}(t)$ in (1) is sampled at rate B to enable discrete-time processing without loss of information. Thus, there are $M = \lfloor TB \rfloor$ samples per symbol. Define the matrix

$$\mathbf{Q}_k \stackrel{\text{def}}{=} \left[\boldsymbol{\psi}_k(0), \boldsymbol{\psi}_k\left(\frac{1}{B}\right), \ldots, \boldsymbol{\psi}_k\left(\frac{M-1}{B}\right)\right]^T \tag{7}$$

whose rows are time-delayed versions of the code of the kth user. Sampling the received signal (1) generates the $R \times M$ matrix

$$\underbrace{\left[\mathbf{r}(0), \mathbf{r}\left(\frac{1}{B}\right), \ldots, \mathbf{r}\left(\frac{M-1}{B}\right)\right]}_{\boldsymbol{\mathcal{R}}} = \sum_{k=1}^{K} b_k \sqrt{\rho_k} \mathbf{A}_k \mathbf{H}_k \mathbf{Q}_k^T + \left[\mathbf{n}(0), \mathbf{n}\left(\frac{1}{B}\right), \ldots, \mathbf{n}\left(\frac{M-1}{B}\right)\right]. \tag{8}$$

Let $\mathbf{r} \stackrel{\text{def}}{=} \text{vec}(\boldsymbol{\mathcal{R}})$ and $\mathbf{h}_k \stackrel{\text{def}}{=} \text{vec}(\mathbf{H}_k)$ be the RM-dimensional vectorized received signal and channel coefficients, respectively. Here, $\text{vec}(\mathbf{X})$ denotes a vector formed by stacking the columns of matrix $\mathbf{X}$ into a vector [21]. Using the identity $\text{vec}(\mathbf{AXB}) = (\mathbf{B}^T \otimes \mathbf{A})\text{vec}(\mathbf{X})$ where $\otimes$ denotes the Kronecker matrix product [21], we may write $\mathbf{r}$ as

$$\mathbf{r} = \underbrace{b_1 \mathbf{B}_1 \mathbf{h}_1}_{\text{desired signal}} + \underbrace{\sum_{k=2}^{K} b_k \sqrt{\rho_k}\, \mathbf{B}_k \mathbf{h}_k}_{\text{MAI}} + \mathbf{n}. \tag{9}$$

$\mathbf{Q}_k$ and $\mathbf{A}_k$ have full column rank and the columns of $\mathbf{B}_k \stackrel{\text{def}}{=} \mathbf{Q}_k \otimes \mathbf{A}_k$ form the *canonical space–time basis* for the received signal of user k. Note that the basis functions are separable in space and time. These basis functions correspond to the CSTCs of the kth user. The number of columns is $N_k = (P_k^+ - P_k^- + 1) \times (L_k + 1) < RM$, where RM is the dimension of the space–time signal space. We note that the space–time basis functions are fixed *a priori* and do not depend on channel parameters—all information about the channel is contained in the coefficients $\mathbf{h}_k$.

A. Active and Inactive Coordinates

The canonical signal representation (9) states that the signal of the kth user belongs to an N_k-dimensional subspace of $\mathbb{C}^{RM}$ determined by the space–time channel spread seen by the user. The CSTCs of each user provide a natural partitioning of the signal space into *active* and *inactive* coordinates. The *active* coordinates correspond to the space–time basis functions that lie within the user's channel spread and carry all the energy of the user's signal as well as MAI. The *inactive* coordinates correspond to basis functions that lie outside the channel spread and thus contain mostly MAI. As we will see, this CSTC partitioning into active/inactive coordinates provides a natural and systematic framework for controlling receiver complexity and performance.

The focus in this paper is on decentralized detection assuming that only the signature code of the desired user ($k = 1$) is available at the receiver. Let $\mathbf{X}^\dagger \stackrel{\text{def}}{=} (\mathbf{X}^H\mathbf{X})^{-1}\mathbf{X}^H$ denote the Moore–Penrose pseudoinverse of matrix $\mathbf{X}$ [22]. The mapping of the received signal $\mathbf{r}$ in (9) onto the $N_A = N_1$ active coordinates of the desired user is given by

$$\mathbf{y}_1 \stackrel{\text{def}}{=} \mathbf{B}_1^\dagger \mathbf{r} = b_1\mathbf{h}_1 + \sum_{k=2}^{K} b_k\sqrt{\rho_k}(\mathbf{B}_1^H\mathbf{B}_1)^{-1}\mathbf{B}_1^H\mathbf{B}_k\mathbf{h}_k + \boldsymbol{\eta}_1 \tag{10}$$

$$\boldsymbol{\eta}_1 \sim \mathcal{N}_C[\mathbf{0},\, \sigma^2(\mathbf{B}_1^H\mathbf{B}_1)^{-1}]. \tag{11}$$

Using the identities $(\mathbf{X}\otimes\mathbf{Y})^{-1} = \mathbf{X}^{-1}\otimes\mathbf{Y}^{-1}$ and $\mathbf{X}_1\mathbf{Y}_1 \otimes \mathbf{X}_2\mathbf{Y}_2 = (\mathbf{X}_1\otimes\mathbf{X}_2)(\mathbf{Y}_1\otimes\mathbf{Y}_2)$, it can be shown that

$$\mathbf{y}_1 = b_1\mathbf{h}_1 + \sum_{k=2}^{K} b_k\sqrt{\rho_k}(\mathbf{Q}_1^\dagger\mathbf{Q}_k \otimes \mathbf{A}_1^\dagger\mathbf{A}_k)\mathbf{h}_k + \boldsymbol{\eta}_1 \tag{12}$$

$$\boldsymbol{\eta}_1 \sim \mathcal{N}_C[\mathbf{0},\, \sigma^2(\mathbf{Q}_1^H\mathbf{Q}_1)^{-1} \otimes (\mathbf{A}_1^H\mathbf{A}_1)^{-1}] \tag{13}$$

which clearly reveals the dependence of $\mathbf{y}_1$ on the canonical space–time bases of each user. Mapping onto the active CSTCs can be performed separately in space and time; that is, $\mathbf{B}_1^\dagger$ is space–time separable. This property also influences the structure of MAI corrupting the desired user's active coordinates, as we discuss shortly. Note that space–time separability in CSTC mapping does not result in space–time separability of decentralized interference suppression (see Section III, unlike some existing work [12]–[15]).

In the absence of MAI, the active coordinates provide sufficient statistics for detection—the maximal ratio combining (MRC) receiver can be implemented by correlating $\mathbf{y}_A$ with $\mathbf{h}_1$ [16]. While the active coordinates completely capture the desired user signal, it will be demonstrated in Section III that limited MAI suppression can be obtained by utilizing the $N_A < RM$ active coordinates. Additional MAI suppression can be obtained by incorporating a set of N_I *inactive* coordinates that *contain only MAI components*. Inactive coordinates can either be directly obtained from the CSTCs of the desired user by considering the coordinates outside the channel spread, *or* from a subspace of the $(RM - N_A)$-dimensional orthogonal complement of $\mathbf{B}_1$. Correlation between the MAI components in the active and inactive coordinates is exploited to improve the MAI suppression by progressively adding inactive coordinates.

Assume that N_I active coordinates are employed and denote the matrix containing the N_I basis vectors corresponding to these inactive coordinates as $\mathbf{B}_I$. Furthermore, define $\mathbf{B}_A = \mathbf{B}_1$. Analogous to (10), the mapping onto active and inactive coordinates is given as

$$\mathbf{y} = \begin{bmatrix}\mathbf{y}_A \\ \mathbf{y}_I\end{bmatrix} = [\,\mathbf{B}_A \quad \mathbf{B}_I\,]^\dagger\mathbf{r}. \tag{14}$$

Expressions for $\mathbf{y}_A$ and $\mathbf{y}_I$ can be obtained as follows. Define

$$\boldsymbol{\Omega} = \begin{bmatrix}\boldsymbol{\Omega}_{AA} & \boldsymbol{\Omega}_{AI} \\ \boldsymbol{\Omega}_{AI}^H & \boldsymbol{\Omega}_{II}\end{bmatrix} \stackrel{\text{def}}{=} \begin{bmatrix}\mathbf{B}_A^H\mathbf{B}_A & \mathbf{B}_A^H\mathbf{B}_I \\ \mathbf{B}_I^H\mathbf{B}_A & \mathbf{B}_I^H\mathbf{B}_I\end{bmatrix}. \tag{15}$$

Use the block matrix inverse formula and the matrix inversion lemma [22]

$$(\mathbf{A}+\mathbf{BCD})^{-1} = \mathbf{A}^{-1} - \mathbf{A}^{-1}\mathbf{B}(\mathbf{DA}^{-1}\mathbf{B}+\mathbf{C}^{-1})^{-1}\mathbf{DA}^{-1} \tag{16}$$

to show from (9) and (14) that

$$\mathbf{y}_A = b_1\mathbf{h}_1 + \sum_{k=2}^{K} b_k\sqrt{\rho_k}\,\mathbf{K}_{A,\,k}\mathbf{h}_k + \boldsymbol{\eta}_A \tag{17}$$

$$\mathbf{y}_I = \sum_{k=2}^{K} b_k\sqrt{\rho_k}\,\mathbf{K}_{I,\,k}\mathbf{h}_k + \boldsymbol{\eta}_I \tag{18}$$

where

$$\begin{aligned}
\mathbf{K}_{A,\,k} &= (\boldsymbol{\Omega}_{AA} - \boldsymbol{\Omega}_{AI}\boldsymbol{\Omega}_{II}^{-1}\boldsymbol{\Omega}_{AI}^H)^{-1}\mathbf{B}_A^H\mathbf{B}_k \\
&\quad - \boldsymbol{\Omega}_{AA}^{-1}\boldsymbol{\Omega}_{AI}(\boldsymbol{\Omega}_{II} - \boldsymbol{\Omega}_{AI}^H\boldsymbol{\Omega}_{AA}^{-1}\boldsymbol{\Omega}_{AI})^{-1}\mathbf{B}_I^H\mathbf{B}_k \\
\mathbf{K}_{I,\,k} &= (\boldsymbol{\Omega}_{II} - \boldsymbol{\Omega}_{AI}^H\boldsymbol{\Omega}_{AA}^{-1}\boldsymbol{\Omega}_{AI})^{-1}\mathbf{B}_I^H\mathbf{B}_k \\
&\quad - (\boldsymbol{\Omega}_{II} - \boldsymbol{\Omega}_{AI}^H\boldsymbol{\Omega}_{AA}^{-1}\boldsymbol{\Omega}_{AI})^{-1}\boldsymbol{\Omega}_{AI}^H\boldsymbol{\Omega}_{AA}^{-1}\mathbf{B}_A^H\mathbf{B}_k \\
\boldsymbol{\eta}_A &\sim \mathcal{N}_C[\mathbf{0},\, \sigma^2(\boldsymbol{\Omega}_{AA} - \boldsymbol{\Omega}_{AI}\boldsymbol{\Omega}_{II}^{-1}\boldsymbol{\Omega}_{AI}^H)^{-1}] \\
\boldsymbol{\eta}_I &\sim \mathcal{N}_C[\mathbf{0},\, \sigma^2(\boldsymbol{\Omega}_{II} - \boldsymbol{\Omega}_{AI}^H\boldsymbol{\Omega}_{AA}^{-1}\boldsymbol{\Omega}_{AI})^{-1}] \\
\mathrm{E}[\boldsymbol{\eta}_A\boldsymbol{\eta}_I^H] &= -\sigma^2\boldsymbol{\Omega}_{AA}^{-1}\boldsymbol{\Omega}_{AI}(\boldsymbol{\Omega}_{II} - \boldsymbol{\Omega}_{AI}^H\boldsymbol{\Omega}_{AA}^{-1}\boldsymbol{\Omega}_{AI})^{-1}.
\end{aligned} \tag{19}$$

The mapping of $\mathbf{r}$ onto the active and inactive canonical coordinates is illustrated in Fig. 1. This mapping essentially decomposes the received signal $\mathbf{r}$ into two components, one which contains the desired user signal, and the other with no desired user signal. The absence of desired signal in inactive coordinates $\mathbf{B}_I$ is evident from (18). "Leakage" of the desired user signal into inactive coordinates is prevented by the pseudoinverse operation in (14).

Note that $\mathbf{y}_A$ is *not* equal to $\mathbf{y}_1$ in (10) unless $\mathbf{B}_I^H\mathbf{B}_A = \mathbf{0}$, i.e., $\mathbf{B}_I$ is chosen from the orthogonal complement of $\mathbf{B}_A$. In this case, (19) can be simplified as follows:

$$\mathbf{K}_{A,\,k} = \mathbf{B}_A^\dagger\mathbf{B}_k, \qquad \mathbf{K}_{I,\,k} = \mathbf{B}_I^\dagger\mathbf{B}_k \tag{20}$$

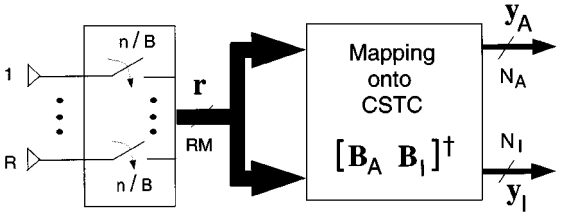

Fig. 1. Mapping the RN-dimensional received signal onto active ($\mathbf{y}_A$) and inactive ($\mathbf{y}_I$) CSTCs.

with $\boldsymbol{\eta}_A \sim \mathcal{N}_C[\mathbf{0}, \sigma^2(\mathbf{B}_A^H\mathbf{B}_A)^{-1}]$, $\boldsymbol{\eta}_I \sim \mathcal{N}_C[\mathbf{0}, \sigma^2(\mathbf{B}_I^H\mathbf{B}_I)^{-1}]$, and $\mathrm{E}[\boldsymbol{\eta}_A\boldsymbol{\eta}_I^H] = \mathbf{0}$. Choosing $\mathbf{B}_I$ from the CSTCs of the desired user outside its channel spread is perhaps most natural, although this choice does not generally satisfy $\mathbf{B}_I^H\mathbf{B}_A = \mathbf{0}$ because time-shifted versions of the desired user's code are generally not orthogonal. Note that $[\mathbf{B}_A \quad \mathbf{B}_I]^\dagger$ may be computed off-line once the channel spreads are known.

B. Structure of Interference in the Desired User's CSTCs

We now study how MAI is distributed throughout the desired user's canonical coordinates. Consider the noise-free received signal vector $\mathbf{r}$ in (9). Denote the *full* RM-dimensional space–time basis generated from the *entire* set of desired user's CSTCs $\{(\phi, \tau) \in \{\varphi_1, \ldots, \varphi_R\} \times \{0, 1/B, \ldots, M-1/B\}\}$ as $\mathbf{B} = \mathbf{Q} \otimes \mathbf{A}$. Note that $\mathbf{Q}$ and $\mathbf{A}$ are $M \times M$ and $R \times R$ nonsingular matrices, respectively. For illustrative purposes, we assume a linear equally spaced array, with $\lambda/2$ element spacing, and choose $\{\varphi_p\}_{p=1}^R = \sin^{-1}\{-(R-1)/R, -(R-3)/R, \ldots, (R-3)/R, (R-1)/R\}$ in (3) so that $\{\mathbf{a}(\varphi_p)\}_{p=1}^R$ form a set of orthonormal spatial basis vectors.

Define $\mathbf{y} = \mathbf{B}^\dagger\mathbf{r} = \mathbf{y}_s + \mathbf{y}_i$, where $\mathbf{y}_s$ and $\mathbf{y}_i$ are the desired signal and MAI mapped onto the full dimensional basis of the desired user, respectively. Similar to (10), $\mathbf{y}_s$ has at most N_A nonzero components corresponding to the desired user's channel vector $\mathbf{h}_1$. The interference component $\mathbf{y}_i$ takes the following form:

$$\mathbf{y}_i = \sum_{k=2}^{K} b_k\sqrt{\rho_k}(\mathbf{Q}^{-1}\mathbf{Q}_k \otimes \mathbf{A}^H\mathbf{A}_k)\mathbf{h}_k. \tag{21}$$

Some insight about the MAI distribution throughout the CSTCs of the desired user can be gained from (21). The MAI distribution in the temporal direction is dictated by the correlation properties of the desired and interfering user spreading codes (as measured by $\mathbf{Q}^{-1}\mathbf{Q}_k$). Due to the pseudorandom characteristics of the spreading codes, $\mathbf{Q}^{-1}\mathbf{Q}_k$ is not sparse, in general. Hence, the MAI component is generally nonzero along the entire temporal (delay) axis. While the spreading codes are different for different users, the same array response vector $\mathbf{a}(\phi)$ applies to all users. This implies that $\mathbf{A}_k$ is a submatrix of $\mathbf{A}$, and by the orthonormality condition, the components of $\mathbf{y}_i$ are zero *outside* $\phi \in \sin^{-1}\{\min_{k=2,\ldots,K}(\varphi_{P_k^-}), \ldots, \max_{k=2,\ldots,K}(\varphi_{P_k^+})\}$. Thus, inactive coordinates corresponding to

$$(\phi, \tau) \in \sin^{-1}\left\{\min_{k=2,\ldots,K}\left(\varphi_{P_k^-}\right), \ldots, \max_{k=2,\ldots,K}\left(\varphi_{P_k^+}\right)\right\} \times \{0, 1/B, \ldots, (M-1)1/B\} \tag{22}$$

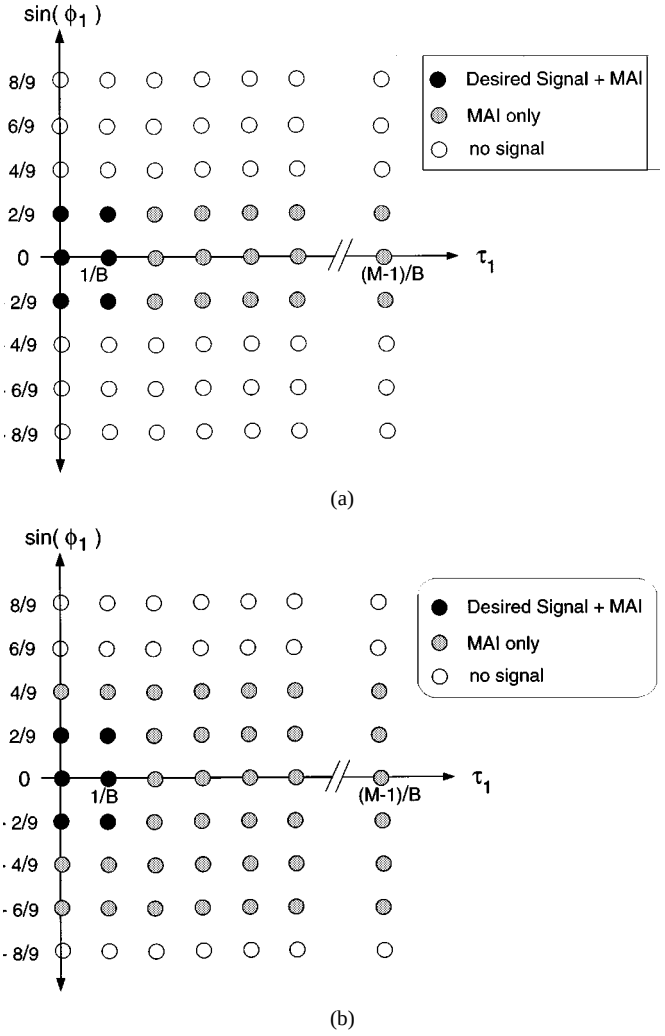

Fig. 2. Distribution of signal $\mathbf{y}_s$ and interference $\mathbf{y}_i$ within the desired user CSTC for uplink assuming $R = 9$, $L_1 = 1$, $\sin\varphi_{P_1^+} = 2/9$, $\sin\varphi_{P_1^-} = -2/9$. (a) Nine-sensor, downlink. (b) Nine-sensor, uplink: $\max_{k=2,\ldots,K}(\sin\varphi_{P_k^+}) = 4/9$ and $\min_{k=2,\ldots,K}(\sin\varphi_{P_k^-}) = -6/9$.

generally contain MAI. The columns of $\mathbf{A}$ can be viewed as beamformers, so the only spatial coordinates containing significant MAI correspond to beams pointed within the angular spread of the interferers. When the number of interfering users is reasonably large and users are widely distributed spatially, as is the case in the uplink of a cellular system, most of the angular components would contain MAI. In the downlink, the signals from all users share the same channel spread and coefficients. Thus, in the spatial direction the MAI is confined only to the active coordinates. While there is no distinction between the active and inactive coordinates spatially, the MAI is distributed all over the temporal axis due to the different signature codes of users. Hence, in the downlink of a cellular system, only the temporal inactive coordinates within the spatial spread of the desired user can be exploited for MAI suppression.

We illustrate the distribution of MAI throughout the desired user angle-delay plane in Fig. 2(a) and (b) for downlink and uplink scenarios, respectively. A nine-sensor receiver with no background noise present is used with the desired user channel spread $L_1 = 1$, $\sin\varphi_{P_1^+} = 2/9$, and $\sin\varphi_{P_1^-} = -(2/9)$.

For the uplink, $\max_{k=2,\ldots,K}(\sin\varphi_{P_k^+}) = 4/9$ and $\min_{k=2,\ldots,K}(\sin\varphi_{P_k^-}) = -(6/9)$. The above examples are merely for illustrative purposes. For current cellular systems, the angular spread in the downlink scenario is typically close to π due to the presence of scatterers all around the mobile handsets. In the uplink scenario, the angular spreads tend to be fairly small due to the elevated position of the base station array.

III. Coherent Decentralized Multiuser Detection

In this section, we discuss linear decentralized multiuser detectors for antipodal signaling. For simplicity, we assume $(\tau_1 + T_1) \ll T$. Hence intersymbol interference (ISI) is negligible and a one-symbol detector suffices. The detector takes the form $\hat{b}_1 = \text{sign}(\text{Re}\{Z\})$, where the decision statistic $Z = \mathbf{g}^H\mathbf{y}$. The combiner $\mathbf{g}$ is designed to perform MAI-resistant coherent combining of N_A active coordinates, while utilizing N_I inactive coordinates to enhance MAI suppression. The choice of $\mathbf{g}$ is based on minimizing the mean squared error (MSE) in estimating b_1. The set of inactive coordinates is chosen from those containing MAI components.

Before proceeding, define data covariance matrix $\mathbf{R}_{yy} = \text{E}[\mathbf{y}\mathbf{y}^H]$. We employ two distinct partitions of $\mathbf{R}_{yy}$:

$$\mathbf{R}_{yy} = \mathbf{R}_{ss} + \mathbf{R}_{nn} \tag{23}$$

and

$$\mathbf{R}_{yy} = \begin{bmatrix} \text{E}[\mathbf{y}_A\mathbf{y}_A^H] & \text{E}[\mathbf{y}_A\mathbf{y}_I^H] \\ \text{E}[\mathbf{y}_I\mathbf{y}_A^H] & \text{E}[\mathbf{y}_I\mathbf{y}_I^H] \end{bmatrix} = \begin{bmatrix} \mathbf{R}_{AA} & \mathbf{R}_{AI} \\ \mathbf{R}_{AI}^H & \mathbf{R}_{II} \end{bmatrix}. \tag{24}$$

In (23), $\mathbf{R}_{yy}$ is partitioned into the desired signal component $\mathbf{R}_{ss}$ and MAI-plus-noise component $\mathbf{R}_{nn}$, whereas (24) partitions $\mathbf{R}_{yy}$ in terms of active and inactive coordinates. In addition, define

$$\mathbf{c}_1 = \begin{bmatrix} \mathbf{h}_1 \\ \mathbf{0} \end{bmatrix} \tag{25}$$

$$\mathbf{G} = \begin{bmatrix} \mathbf{G}_A \\ \mathbf{G}_I \end{bmatrix} = \begin{bmatrix} \sqrt{\rho_2}\,\mathbf{B}_A^H\mathbf{B}_2\mathbf{h}_2 \cdots \sqrt{\rho_K}\,\mathbf{B}_A^H\mathbf{B}_K\mathbf{h}_K \\ \sqrt{\rho_2}\,\mathbf{B}_I^H\mathbf{B}_2\mathbf{h}_2 \cdots \sqrt{\rho_K}\,\mathbf{B}_I^H\mathbf{B}_K\mathbf{h}_K \end{bmatrix} \tag{26}$$

where $\mathbf{B}_A$, $\mathbf{B}_I$, and $\mathbf{B}_k$ are defined in (14) and (9).

Let T_s denote the duration over which $\mathbf{R}_{yy}$ is estimated. We assume that T_s is smaller than the coherence time of the desired user's channel which implies that the channel coefficient vector $\mathbf{h}_1$ is approximately constant over the duration T_s. It follows from (17) to (26) that

$$\mathbf{R}_{ss} = \mathbf{c}_1\mathbf{c}_1^H, \quad \mathbf{R}_{nn} = \mathbf{\Omega}^{-1}\text{E}[\mathbf{G}\mathbf{G}^H]\mathbf{\Omega}^{-1} + \sigma^2\mathbf{\Omega}^{-1} \tag{27}$$

where $\text{E}[\mathbf{G}\mathbf{G}^H] = [\mathbf{B}_A \quad \mathbf{B}_I]^H \left(\sum_{k=2}^K \mathbf{B}_k\text{E}[\mathbf{h}_k\mathbf{h}_k^H]\mathbf{B}_k^H\right) [\mathbf{B}_A \quad \mathbf{B}_I]$ and Ω is defined in (15).

The LCMV technique can be applied to design the MMSE combiner $\mathbf{g} = [\mathbf{g}_A^T \quad \mathbf{g}_I^T]^T$:

$$\begin{aligned} \mathbf{g} &= \arg\min_{\mathbf{w}} \text{E}|\mathbf{w}^H\mathbf{y}|^2 \qquad s.t.\ \mathbf{w}^H\mathbf{c}_1 = 1 \\ &= \frac{\mathbf{R}_{yy}^{-1}\mathbf{c}_1}{\mathbf{c}_1^H\mathbf{R}_{yy}^{-1}\mathbf{c}_1} = \frac{\mathbf{R}_{nn}^{-1}\mathbf{c}_1}{\mathbf{c}_1^H\mathbf{R}_{nn}^{-1}\mathbf{c}_1} \end{aligned} \tag{28}$$

where $\mathbf{c}_1$ is defined in (25) and the second equality in (28) is obtained by applying (16) to (23). Note that $\mathbf{g}$ utilizes one of $N_T = N_A + N_I$ available dimensions to coherently combine the desired signal component in $\mathbf{y}$ while suppressing the MAI using the remaining $N_A + N_I - 1$ dimensions. An equivalent formulation of (28) that directly provides explicit forms for $\mathbf{g}_A$ and $\mathbf{g}_I$ is given by

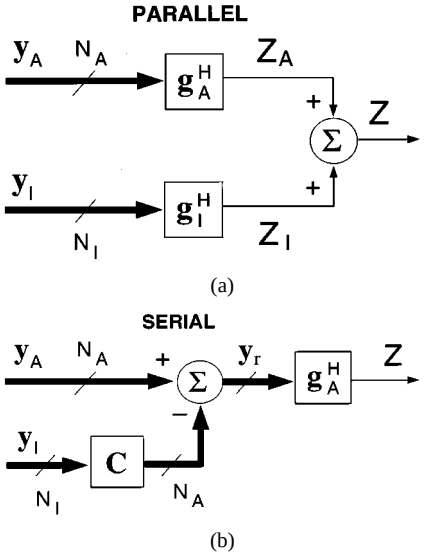

Fig. 3. (a) Parallel and (b) serial MAI canceler.

$$\begin{bmatrix} \mathbf{g}_A \\ \mathbf{g}_I \end{bmatrix} = \arg\min_{\mathbf{w}_A, \mathbf{w}_I} \text{E}|\mathbf{w}_A^H\mathbf{y}_A + \mathbf{w}_I^H\mathbf{y}_I|^2 \quad s.t.\ \mathbf{w}_A^H\mathbf{h}_1 = 1 \tag{29}$$

$$= \begin{bmatrix} \mathbf{I}_{N_A} \\ -\mathbf{R}_{II}^{-1}\mathbf{R}_{AI}^H \end{bmatrix} \frac{(\mathbf{R}_{AA} - \mathbf{R}_{AI}\mathbf{R}_{II}^{-1}\mathbf{R}_{AI}^H)^{-1}\mathbf{h}_1}{\mathbf{h}_1^H(\mathbf{R}_{AA} - \mathbf{R}_{AI}\mathbf{R}_{II}^{-1}\mathbf{R}_{AI}^H)^{-1}\mathbf{h}_1}. \tag{30}$$

The solution given in (30) can be easily derived using the Lagrangian of (29) with respect to $\mathbf{w}_A$ and $\mathbf{w}_I$. We term this the *parallel* structure since the active and inactive coordinates are processed in parallel, as depicted in Fig. 3(a). Notice that $\mathbf{g}^H = \mathbf{g}_A^H[\mathbf{I}_{N_A} - \mathbf{C}]$, where $\mathbf{C} = \mathbf{R}_{AI}\mathbf{R}_{II}^{-1}$. This suggests a *serial* structure for implementing the detector depicted in Fig. 3(b). In the serial structure, $\mathbf{C}$ uses the inactive coordinates to suppress the MAI components in the active coordinates by forming $\mathbf{y}_r = \mathbf{y}_A - \mathbf{C}\mathbf{y}_I$, and then the remaining MAI in $\mathbf{y}_r$ is further suppressed by $\mathbf{g}_A$. Equivalently, $\mathbf{C}$ and $\mathbf{g}_A$ solve the sequential optimization problems

$$\mathbf{C} = \arg\min_{\mathbf{W}} \text{E}\|\mathbf{y}_A - \mathbf{W}\mathbf{y}_I\|^2 = \mathbf{R}_{AI}\mathbf{R}_{II}^{-1} \tag{31}$$

$$\mathbf{g}_A = \arg\min_{\mathbf{w}:\, s.t.\ \mathbf{w}^H\mathbf{h}_1 = 1} \text{E}|\mathbf{w}^H\mathbf{y}_r|^2 = \mathbf{R}_{y_ry_r}^{-1}\mathbf{h}_1/\mathbf{h}_1^H\mathbf{R}_{y_ry_r}^{-1}\mathbf{h}_1 \tag{32}$$

where it can be shown that $\mathbf{R}_{y_ry_r} = \text{E}[\mathbf{y}_r\mathbf{y}_r^H] = \mathbf{R}_{AA} - \mathbf{R}_{AI}\mathbf{R}_{II}^{-1}\mathbf{R}_{AI}^H$.

The equivalence between serial and parallel structures applies even when the true covariance matrices are replaced by estimated covariance matrices. Hence, the adaptive convergence properties of serial and parallel structures are identical for any adaptive algorithm based on estimated covariance matrices. However, as discussed later, the serial structure is advantageous for blind channel estimation and noncoherent detection.

IV. Performance Analysis

We assume that $\mathbf{h}_1$ is perfectly known and $\mathbf{g}$ is given by (30). The test statistic Z can be decomposed as $Z = Z_s + Z_{in}$, where Z_s contains the desired signal and Z_{in} contains the MAI and noise. This leads to the definition of signal-to-interference-and-noise ratio (SINR) as

$$\text{SINR} = \frac{\mathrm{E}|Z_s|^2}{\mathrm{E}|Z_{in}|^2} = \frac{\mathbf{g}^H \mathbf{R}_{ss} \mathbf{g}}{\mathbf{g}^H \mathbf{R}_{nn} \mathbf{g}} = \mathbf{c}_1^H \mathbf{R}_{nn}^{-1} \mathbf{c}_1. \tag{33}$$

Define $D \leq N_T$ to be the *effective* rank of the interference portion of $\mathbf{R}_{nn}$ in (27), which is $\mathbf{\Omega}^{-1}\mathrm{E}[\mathbf{G}\mathbf{G}^H]\mathbf{\Omega}^{-1}$. Consider the factorization

$$\mathrm{E}[\mathbf{G}\mathbf{G}^H] = \mathbf{\Gamma}\mathbf{\Gamma}^H \tag{34}$$

where $\mathbf{\Gamma}$ is an $N_T \times D$ full column rank matrix. Applying (16) to $\mathbf{R}_{nn}$ in (27), we obtain

$$\mathbf{R}_{nn}^{-1} = \mathbf{\Omega}(\mathbf{\Gamma}\mathbf{\Gamma}^H + \sigma^2\mathbf{\Omega})^{-1}\mathbf{\Omega} \tag{35}$$

$$= \sigma^{-2}[\mathbf{\Omega} - \mathbf{\Gamma}(\mathbf{\Gamma}^H\mathbf{\Omega}^{-1}\mathbf{\Gamma} + \sigma^2\mathbf{I})^{-1}\mathbf{\Gamma}^H]. \tag{36}$$

It follows from (33) and (36) that the SINR of the detector can be written as follows:

$$\text{SINR} = \frac{\mathbf{c}_1^H\mathbf{\Omega}\mathbf{c}_1}{\sigma^2}\left[1 - \frac{\mathbf{c}_1^H\mathbf{\Gamma}(\mathbf{\Gamma}^H\mathbf{\Omega}^{-1}\mathbf{\Gamma} + \sigma^2\mathbf{I})^{-1}\mathbf{\Gamma}^H\mathbf{c}_1}{\mathbf{c}_1^H\mathbf{\Omega}\mathbf{c}_1}\right]. \tag{37}$$

Observe that the first product term in (37), $\mathbf{c}_1^H\mathbf{\Omega}\mathbf{c}_1/\sigma^2$, is the SINR when MAI is absent. The second term, in brackets, represents a loss factor due to the presence of MAI which depends on the overlap between the desired signal and MAI subspaces, as well as the interference and noise power. The use of inactive coordinates facilitates suppression of MAI within the active coordinates and thus improves SINR. In fact, as shown in the Appendix, the SINR increases monotonically as the number of inactive coordinates is increased.

We now investigate the behavior of SINR in various asymptotic regimes. First of all, $\mathbf{g}$ reduces to the single-user MRC detector in the absence of MAI since $\mathbf{R}_{nn}^{-1} = \mathbf{\Omega}$ in this case. Another case of interest is when the interferer powers increase without bound. Define $\mathbf{P}_\Gamma^\perp = \mathbf{I} - \mathbf{\Omega}^{-1/2}\mathbf{\Gamma}(\mathbf{\Gamma}^H\mathbf{\Omega}^{-1}\mathbf{\Gamma})^{-1}\mathbf{\Gamma}^H\mathbf{\Omega}^{-1/2}$, which is the projection matrix orthogonal to the MAI space. Let all interferer powers increase at the same rate ($\rho_k = \rho \uparrow \infty$). Define $\mathbf{\Gamma}_u = \mathbf{\Gamma}/\sqrt{\rho}$, which is the MAI matrix with the *common* interfering user power term factored out, and note that $\mathbf{P}_{\Gamma_u}^\perp = \mathbf{P}_\Gamma^\perp$. The following results can be derived using (16):

$$\lim_{\rho_2 = \cdots = \rho_K \uparrow \infty} \text{SINR} = \begin{cases} 0, & D = N_T \\ \sigma^{-2}\left\|\mathbf{P}_{\Gamma_u}^\perp \mathbf{\Omega}^{1/2}\mathbf{c}_1\right\|^2, & D < N_T \end{cases} \tag{38}$$

$$\lim_{\rho_2 = \cdots = \rho_K \uparrow \infty} \mathbf{g} = \begin{cases} \mathbf{\Omega}(\mathbf{\Gamma}_u\mathbf{\Gamma}_u^H)^{-1}\mathbf{\Omega}\mathbf{c}_1 / \mathbf{c}_1^H\mathbf{\Omega}(\mathbf{\Gamma}_u\mathbf{\Gamma}_u^H)^{-1}\mathbf{\Omega}\mathbf{c}_1, & D = N_T, \\ \mathbf{\Omega}^{1/2}\mathbf{P}_{\Gamma_u}^\perp \mathbf{\Omega}^{1/2}\mathbf{c}_1 \Big/ \left\|\mathbf{P}_{\Gamma_u}^\perp \mathbf{\Omega}^{1/2}\mathbf{c}_1\right\|^2, & D < N_T. \end{cases} \tag{39}$$

The above results imply that, when $D < N_T$, the combiner $\mathbf{g}$ converges to the decorrelating detector as $\rho_2 = \cdots = \rho_K \uparrow \infty$. That is, the output interference signal goes to zero while the desired user sees unit gain, as shown by

$$\lim_{\rho_2 = \cdots = \rho_K \uparrow \infty} \mathbf{g}^H\mathbf{\Omega}^{-1}\mathbf{\Gamma} = \frac{\mathbf{c}_1^H\mathbf{\Omega}^{1/2}}{\|\mathbf{P}_\Gamma^\perp\mathbf{\Omega}^{1/2}\mathbf{c}_1\|^2}\mathbf{P}_\Gamma^\perp\mathbf{\Omega}^{-1/2}\mathbf{\Gamma} = \mathbf{0}^H$$

$$\lim_{\rho_2 = \cdots = \rho_K \uparrow \infty} \mathbf{g}^H\mathbf{c}_1 = \frac{\mathbf{c}_1^{-1}\mathbf{\Omega}^{1/2}\mathbf{P}_\Gamma^\perp\mathbf{\Omega}^{1/2}\mathbf{c}_1}{\|\mathbf{P}_\Gamma^\perp\mathbf{\Omega}^{1/2}\mathbf{c}_1\|^2} = 1 \tag{40}$$

where $\mathbf{\Omega}^{-1}\mathbf{\Gamma}$ and $\mathbf{c}_1$ represent the MAI subspace and the desired signal component in $\mathbf{y}$, respectively. It is important to note that, although $\mathbf{g}$ completely cancels the MAI component as $\rho_2, \ldots, \rho_K \uparrow \infty$, the component of the desired signal in the MAI subspace is also cancelled. This can be seen from (38) since

$$\lim_{\rho_2, \ldots, \rho_K \uparrow \infty} \text{SINR} = \sigma^{-2}\|\mathbf{P}_\Gamma^\perp\mathbf{\Omega}^{1/2}\mathbf{c}_1\|^2 \leq \sigma^{-2}\|\mathbf{\Omega}^{1/2}\mathbf{c}_1\|^2 \tag{41}$$

where $\sigma^{-2}\|\mathbf{\Omega}^{1/2}\mathbf{c}_1\|^2$ is the SINR in the absence of MAI. This inequality follows from the contraction property of projection matrices [22].

Another metric of interest is *near–far resistance*, which is defined in [23] as follows:

$$NFR = \inf_{\rho_2, \ldots, \rho_K} \sup\left\{0 \leq r \leq 1 \colon \lim_{\sigma \to 0} P_e(\sigma) \Big/ Q\left(\sqrt{r \times \frac{\mathbf{c}_1^H\mathbf{\Omega}\mathbf{c}_1}{\sigma^2}}\right) = 0\right\} \tag{42}$$

where $P_e(\sigma)$ is the probability of error as a function of σ. Near–far resistance measures how well the detector performs in the presence of MAI relative to its performance in the absence of MAI, evaluated for the worst-case interference power. Analogous to [1], it can be computed from (42) and (38) to be

$$NFR = \begin{cases} \mathbf{c}_1^H\mathbf{\Omega}^{1/2}\mathbf{P}_\Gamma^\perp\mathbf{\Omega}^{1/2}\mathbf{c}_1 / \mathbf{c}_1^H\mathbf{\Omega}\mathbf{c}_1, & N_T > D \\ 0, & N_T \leq D \end{cases} \tag{43}$$

$$= \frac{\sigma^2}{\mathbf{c}_1^H\mathbf{\Omega}\mathbf{c}_1} \times \lim_{\rho_2, \ldots, \rho_K \uparrow \infty} \text{SINR} \tag{44}$$

where (44) follows from (38). That is, near–far resistance in this case is completely characterized by the asymptotic properties of the SINR. Hence, we have

$$D \leq N_T - 1 \;\Leftrightarrow\; NFR > 0. \tag{45}$$

It is particularly instructive to study the two-user case (assuming that $N_A > K - 1 = 1$) where

$$NFR = 1 - \frac{\left|\mathbf{c}_1^H\begin{bmatrix}\mathbf{B}_A^H\mathbf{B}_2 \\ \mathbf{B}_I^H\mathbf{B}_2\end{bmatrix}\mathbf{h}_2\right|^2}{(\mathbf{h}_2^H\mathbf{J}_2\mathbf{h}_2)(\mathbf{c}_1^H\mathbf{\Omega}\mathbf{c}_1)}$$

$$\mathbf{J}_2 = \mathbf{B}_2^H[\mathbf{B}_A \quad \mathbf{B}_I]\mathbf{\Omega}^{-1}\begin{bmatrix}\mathbf{B}_A^H \\ \mathbf{B}_I^H\end{bmatrix}\mathbf{B}_2. \tag{46}$$

If inactive coordinates are not utilized, NFR can be written as

$$NFR = 1 - \frac{|\mathbf{s}_1^H \mathbf{s}_2|^2}{\|\mathbf{s}_1\|^2 \, \|\mathbf{s}_2\|^2} = 1 - \cos^2 \alpha_{12}$$
$$\mathbf{s}_1 = \mathbf{\Omega}_{AA}^{-1/2} \mathbf{\Omega}_{AA} \mathbf{h}_1, \qquad \mathbf{s}_2 = \mathbf{\Omega}_{AA}^{-1/2} \mathbf{B}_A^H \mathbf{B}_2 \mathbf{h}_2 \tag{47}$$

where α_{12} is the angle between the desired signal and MAI component within the active coordinates. Hence, NFR depends on the angle between the desired signal $\mathbf{s}_1$ and the interference $\mathbf{s}_2$. When $N_I > 0$ so that inactive coordinates are incorporated, we have

$$NFR = 1 - \frac{|\tilde{\mathbf{s}}_1^H \tilde{\mathbf{s}}_2|^2}{\|\tilde{\mathbf{s}}_1\|^2 \|\tilde{\mathbf{s}}_2\|^2} = 1 - \cos^2 \tilde{\alpha}_{12}$$
$$= 1 - \frac{|\mathbf{s}_1^H \mathbf{s}_2|^2}{\|\mathbf{s}_1\|^2 (\|\mathbf{s}_2\|^2 + G_I)}$$
$$\tilde{\mathbf{s}}_1 = \mathbf{\Omega}^{-1/2} \mathbf{\Omega} \mathbf{c}_1, \qquad \tilde{\mathbf{s}}_2 = \mathbf{\Omega}^{-1/2} \begin{bmatrix} \mathbf{B}_A^H \mathbf{B}_2 \\ \mathbf{B}_I^H \mathbf{B}_2 \end{bmatrix} \mathbf{h}_2$$
$$G_I = \|(\mathbf{\Omega}_{AI}^H \mathbf{\Omega}_{AA}^{-1} \mathbf{B}_A^H \mathbf{B}_2 - \mathbf{B}_I^H \mathbf{B}_2) \times (\mathbf{\Omega}_{II} - \mathbf{\Omega}_{AI}^H \mathbf{\Omega}_{AA}^{-1} \mathbf{\Omega}_{AI})^{-1/2} \mathbf{h}_2\|^2. \tag{48}$$

Note that G_I is the gain in near–far resistance due to the use of inactive coordinates.

We conclude from the above results that the detector is MAI-resistant (near–far resistant) as long as $D \leq N_T - 1$, where we recall that D is the effective rank of the interference component of $\mathbf{R}_{yy}$. This makes intuitive sense since N_T represents the number of available dimensions that the receiver can use to suppress the MAI. Since the MAI component lies in a D-dimensional space, the receiver needs at least $D+1$ dimensions to suppress the MAI component, while simultaneously preserving the desired user's signal. The value of D depends on the coherence times of the interfering users relative to the duration T_s over which $\mathbf{R}_{yy}$ is estimated. For simplicity, assume that all interfering users have the same channel coherence time. If the coherence time is larger than T_s, each interferer spans a one-dimensional subspace resulting in $D = K-1$. On the other hand, if the coherence time of interfering users is significantly smaller than T_s, each interferer spans a subspace with dimension as large as N_A, resulting in D as large as $D = (K-1)N_A$.

V. Extension to General Binary Signaling

It is straightforward to extend the CSTC receiver to general binary signaling, i.e., $q_1(t) \in \{\theta^{(0)}(t), \theta^{(1)}(t)\}$. One solution is to map $\mathbf{r}$ in (9) onto two CSTC bases $\mathbf{B}^{(0)} = [\mathbf{B}_A^{(0)} \quad \mathbf{B}_I^{(0)}]$ and $\mathbf{B}^{(1)} = [\mathbf{B}_A^{(1)} \quad \mathbf{B}_I^{(1)}]$, corresponding to $\theta^{(0)}(t)$ and $\theta^{(1)}(t)$. Note that the difference between $\mathbf{B}^{(0)}$ and $\mathbf{B}^{(1)}$ only lies in the temporal structure. For each of the two signaling waveforms, inactive coordinates are used to suppress MAI, as shown in Fig. 4. Provided that $\mathbf{B}_A^{(0)}$ and $\mathbf{B}_A^{(1)}$ are close to being orthogonal, the desired signal component in $\mathbf{r}$ is suppressed in the branch corresponding to the incorrect hypothesis. In this case, the number of linearly independent bases used in the receiver is $2(N_A + N_I)$. Alternatively, one can choose $\mathbf{B}_I^{(0)} = \mathbf{B}_I^{(1)} = \mathbf{B}_I$ with $\mathbf{B}_I^H \mathbf{B}_A^{(0)} = \mathbf{0}$ and $\mathbf{B}_I^H \mathbf{B}_A^{(1)} = \mathbf{0}$, which amounts to using $2N_A + N_I$ linearly independent bases. After MAI suppression, $\mathbf{y}_r^{(0)}$ and $\mathbf{y}_r^{(1)}$ as shown in Fig. 4 are processed to detect b_1, depending upon the knowledge of the desired user channel. Coherent detection can be used when an estimate of $\mathbf{h}_1$ is available: $\mathrm{Re}\{\mathbf{g}_A^{(0)H} \mathbf{y}_r^{(0)} - \mathbf{g}_A^{(1)H} \mathbf{y}_r^{(1)}\} \underset{1}{\overset{0}{\gtrless}} \mathcal{T}_c$, where $\mathcal{T}_c$ is a threshold. The combiners $\mathbf{g}_A^{(0)}$ and $\mathbf{g}_A^{(1)}$ are chosen as discussed previously. If the desired user's channel is rapidly fading and a reliable estimate of $\mathbf{h}_1$ is difficult to obtain, one may resort to noncoherent detection: $\mathbf{y}_r^{(1)H} \mathbf{R}_{h_1 h_1}^{-1} \mathbf{y}_r^{(1)} - \mathbf{y}_r^{(0)H} \mathbf{R}_{h_1 h_1}^{-1} \mathbf{y}_r^{(0)} \underset{1}{\overset{0}{\gtrless}} \mathcal{T}_{nc}$, where $\mathbf{R}_{h_1 h_1} = \mathrm{E}[\mathbf{h}_1 \mathbf{h}_1^H]$. When $\mathbf{R}_{h_1 h_1}$ is unknown, a square-law detector can be used.

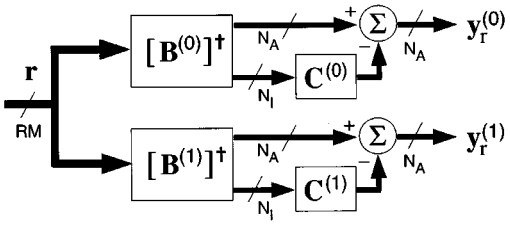

Fig. 4. Front-end decentralized receiver structure for general binary signaling.

VI. Channel Estimation

The desired user's channel $\mathbf{h}_1$ needs to be estimated for implementation of the proposed CSTC receiver. Various MAI-resistant channel estimation techniques described in the literature can be applied within the CSTC framework (see, e.g., [24], [7]). In this paper, we present a blind technique that exploits the serial structure in Fig. 3 [24], [25]. It is straightforward to see that an estimate of $\mathbf{h}_1$ can be obtained from the most dominant eigenvector of $\mathbf{R}_{y_r y_r}$. The accuracy of this estimate depends on the number of inactive coordinates used. Define $\begin{bmatrix} \tilde{\mathbf{\Gamma}}_A \\ \tilde{\mathbf{\Gamma}}_I \end{bmatrix} = \mathbf{\Omega}^{-1} \begin{bmatrix} \mathbf{\Gamma}_A \\ \mathbf{\Gamma}_I \end{bmatrix}$. Then, it can be shown from (24) and (27) that as the noise variance $\sigma^2 \downarrow 0$,

$$\mathbf{R}_{y_r y_r} \to \begin{cases} \mathbf{h}_1 \mathbf{h}_1^H, & N_I \geq D \\ \mathbf{h}_1 \mathbf{h}_1^H + \tilde{\mathbf{\Gamma}}_A \left[\mathbf{I} - \tilde{\mathbf{\Gamma}}_I^H \left(\tilde{\mathbf{\Gamma}}_I \tilde{\mathbf{\Gamma}}_I^H \right)^{-1} \tilde{\mathbf{\Gamma}}_I \right] \tilde{\mathbf{\Gamma}}_A^H, & \\ & N_I < D. \end{cases} \tag{49}$$

Hence, as long as $N_I \geq D$ and σ^2 is small compared to the desired user power, an accurate estimate of $\mathbf{h}_1$ can be obtained up to a phase ambiguity. The phase ambiguity can be removed with the use of differential signaling, or otherwise estimated via pilot-based techniques.

In practice, $\mathbf{R}_{y_r y_r}$ is not known exactly and must be estimated, so only a noisy estimate $\hat{\mathbf{h}}_1 = \mathbf{h}_1 + \mathbf{e}$ is available, where $\mathbf{e}$ denotes the estimation error. It is well known that the LCMV receiver is sensitive to errors in the constraints [2], [26]. In our case, the constraint is $\mathbf{w}_A^H \hat{\mathbf{h}}_1 = 1$. Such errors result in desired signal cancellation since the constraint no longer ensures that the desired user experiences unit gain. This is also observed in [2] due to the presence of multipath. The serial receiver structure offers a solution to this problem: choose $\mathbf{g}_A = \hat{\mathbf{h}}_1$. That is, $\mathbf{g}_A$ is used to implement an MRC without performing any MAI suppression. We term this structure *MRC with cancellation* (C-MRC). In this case, only the inactive coordinates are

utilized for MAI suppression and since $\mathbf{C} = \mathbf{R}_{AI}^H \mathbf{R}_{II}^{-1}$ is independent of $\hat{\mathbf{h}}_1$, cancellation of desired signal does not occur. However, $N_I \geq D$ is required to achieve near–far resistance. It is clear that when the channel estimation error is sufficiently small, selecting $\mathbf{g}_A$ as in (30) results in better performance.

When the error statistics $\mathbf{R}_{ee} = \mathrm{E}[\mathbf{e}\mathbf{e}^H]$ are known, one may use penalized least square (PLS) methods [27], [26] to reduce the sensitivity to channel estimation errors. That is,

$$\mathbf{g} = \arg\min_{\mathbf{w}} \mathrm{E}|\mathbf{w}_A^H \mathbf{y}_A + \mathbf{w}_I^H \mathbf{y}_I|^2 \quad s.t.\ \mathbf{w}_A^H \mathbf{h}_1 = 1, \qquad \mathbf{w}_A^H \mathbf{R}_{ee} \mathbf{w}_A \leq \delta^2. \tag{50}$$

The quadratic constraint is added to prevent excessive desired signal cancellation [27]. It is easy to show that the solution of (50) is

$$\mathbf{g}_A = \frac{(\mathbf{R}_{AA} + \mu \mathbf{R}_{ee} - \mathbf{R}_{AI}\mathbf{R}_{II}^{-1}\mathbf{R}_{AI}^H)^{-1}\hat{\mathbf{h}}_1}{\hat{\mathbf{h}}_1^H (\mathbf{R}_{AA} + \mu \mathbf{R}_{ee} - \mathbf{R}_{AI}\mathbf{R}_{II}^{-1}\mathbf{R}_{AI}^H)^{-1}\hat{\mathbf{h}}_1}, \qquad \mathbf{g}_I = -\mathbf{R}_{II}^{-1}\mathbf{R}_{AI}^H \mathbf{g}_A \tag{51}$$

where $\mu \geq 0$ is a "penalty" parameter chosen to satisfy the quadratic constraint in (50) and is inversely proportional to δ^2. It is shown in [26] that the sensitivity to estimation error decreases monotonically as μ is increased. Increasing μ is equivalent to increasing the background noise level in the active coordinates, so the results in Section IV apply. When the actual $\mathbf{R}_{ee}$ is unknown, one may choose $\mathbf{R}_{ee} = \mathbf{I}_{N_A}$. This reduces the quadratic constraint in (50) to a norm constraint. More detailed discussion of PLS and quadratic constraints can be found in [26] and [27].

VII. Comparison With Chip-Domain Filtering

Most existing space–time receivers employ chip-domain temporal processing (see, e.g., [1], [2]). The received signal is sampled at rate $1/B$ to yield $M = \lfloor TB \rfloor$ temporal samples for each symbol

$$\mathbf{r} = b_1 \mathbf{r}_1 + \sum_{k=1}^{K} b_k \mathbf{r}_k + \mathbf{n} \tag{52}$$

where $\mathbf{r}_k \in \mathbb{C}^{RM}$ is the effective received signature vector for user k and includes the effect of multipath and spatial dispersion. The corresponding LCMV receiver in this case is [1], [2]

$$\tilde{\mathbf{g}} = \arg \min_{\tilde{\mathbf{w}}:\ \tilde{\mathbf{w}}^H \mathbf{r}_1 = 1} \mathrm{E}|\tilde{\mathbf{w}}^H \mathbf{r}|^2 = \frac{\mathbf{R}_{rr}^{-1}\mathbf{r}_1}{\mathbf{r}_1^H \mathbf{R}_{rr}^{-1}\mathbf{r}_1} \tag{53}$$

where $\mathbf{R}_{rr} = \mathrm{E}[\mathbf{r}\mathbf{r}^H]$ and the length of the combiner $\tilde{\mathbf{w}}$ equals the dimension RM of the signal space. In contrast, in the CSTC framework, the signal space partitioning into active and inactive coordinates facilitates lower dimensional processing—the receiver signal is projected onto $N_T = N_A + N_I < RM$ coordinates and processed with a length N_T combiner.

There are three main advantages of CSTC framework over conventional chip-domain filtering. First, in chip-domain filtering, the RM-dimensional the constraint signature vector $\mathbf{r}_1$ needs to be estimated either blindly or from pilot data. In contrast, the CSTC-based LCMV receiver requires estimation of the N_A-dimensional channel coefficient vector $\mathbf{h}_1$. Since $N_A < RM$, CSTC-based receiver requires estimation of a smaller number of desired user channel parameters compared to chip-domain filtering. In the worst case, when the angular spread is π, we have $N_A = R(L_1+1)$ and chip-domain filtering requires a factor of $M/(L_1+1)$ more channel parameters than the CSTC-based approach. This is a significant difference since $L_1 \ll M$ typically. Consequently, the CSTC-based channel estimation requires less data or yields more accurate estimates for a given amount of data. Furthermore, it is well known that estimation error in a parametric model tends to increase with the number of parameters (see, e.g., [22]).

The second advantage of CSTC-based receivers stems from the dimension of the data covariance matrix. While the chip-domain LCMV receiver in (53) requires estimation and inversion of an $RM \times RM$ covariance matrix, the CSTC-based receiver in (30) requires estimation of an $(N_A + N_I) \times (N_A + N_I)$ covariance matrix and inversion of an $N_I \times N_I$ and an $N_A \times N_A$ matrix. Since usually $N_T = N_A + N_I < RM$, the CSTC-based approach has reduced computational requirements and requires less data for covariance matrix estimation. This is a critical advantage since errors in covariance matrix estimation in conventional chip-domain filtering can significantly degrade LCMV receiver performance in mobile scenarios (see, e.g., [7]). To appreciate this difference, consider the concrete example of a wide-band CDMA (WCDMA) system [28] with $R = 1$, spreading gain $M = 128$, and Doppler spread of f_d Hz. It is known that for an N-dimensional random vector, approximately $5N$ independent snapshots are needed to obtain a reasonably accurate estimate of the covariance matrix (see, e.g., [29]). In this case, the receiver in (53) requires approximately 640 independent snapshots to obtain a reliable estimate of $\mathbf{R}_{rr}$. The CSTC-based receiver needs estimates of $\mathbf{R}_{AA}$, $\mathbf{R}_{AI}$, and $\mathbf{R}_{II}$. Assume $N_A < D + 1$. Using the minimum required number of coordinates, $N_T = D + 1$, the CSTC-based scheme requires at most $5(D+1)$ snapshots. In WCDMA, 1 slot (containing 15 symbols) is 625 μs. Hence, the number of symbols within channel coherence time is $24\,000/f_d$ which is approximately the maximum number of snapshots available for covariance matrix estimation. For $f_d = 100$ Hz (mobile speed of 32 mi/h at center frequency 2.15 GHz), about 240 snapshots are available—not enough for chip-domain filtering to yield an accurate covariance matrix estimate. The CSTC-based receiver can obtain accurate estimates of all the required covariance matrices as long as $D \leq 47$, which is possible if on average the number of dominant interferers is less than half the spreading gain.

The third advantage of CSTC framework is related to the C-MRC receiver structure introduced in Section VI. The C-MRC structure provides robustness against channel estimation errors since the MAI suppression does not depend on the channel coefficients. There is no natural analog of C-MRC structure in chip-domain filtering schemes since they do not exploit the notion of active and inactive coordinates.

VIII. Numerical Results

We consider a direct-sequence CDMA system with eight users communicating over a slow multipath fading channel. We consider reception within a coherence time of all users so that the channel coefficients of all users are fixed. The power

TABLE I
MULTIPATH DELAYS AND ANGLES OF ARRIVAL FOR INTERFERING USERS IN EXAMPLES

User	Delays($\times T_c$)	DOA's (rad)
2	{ 0,1,2,3,4 }	$\sin^{-1}\{0, \pm 2/7\}$
3	{ 0,1,2,3,4 }	$\sin^{-1}\{0, \pm 2/7\}$
4	{ 0,1,2,3,4 }	$\sin^{-1}\{0, \pm 2/7\}$
5	{ 1,2,3,4,5,6 }	$\sin^{-1}\{0, \pm 2/7\}$
6	{ 1,2,3,4,5,6 }	$\sin^{-1}\{0, 2/7, 4/7\}$
7	{ 1,2,3,4,5,6 }	$\sin^{-1}\{0, 2/7, 4/7\}$
8	{ 1,2,3,4,5,6 }	$\sin^{-1}\{0, 2/7, 4/7\}$

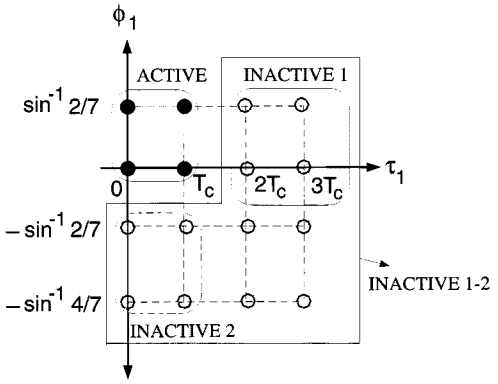

(a)

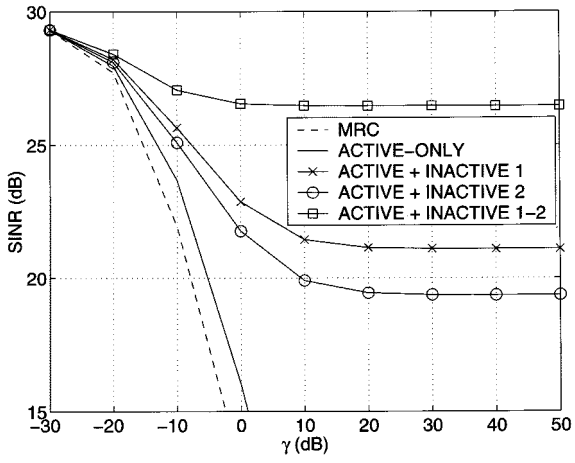

(a)

Fig. 5. Example 1. A seven-sensor eight-user uplink system. (a) Active and inactive coordinate sets. (b) SINR as a function of interference powers.

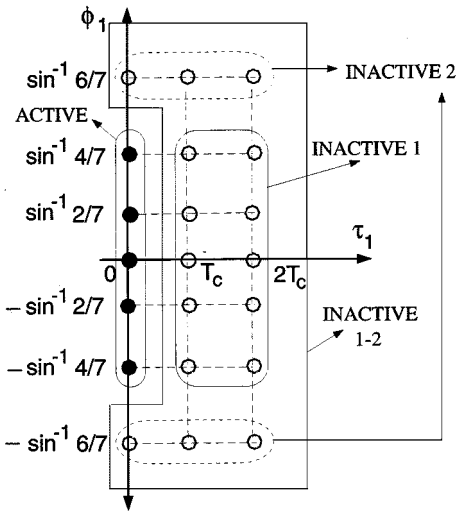

(a)

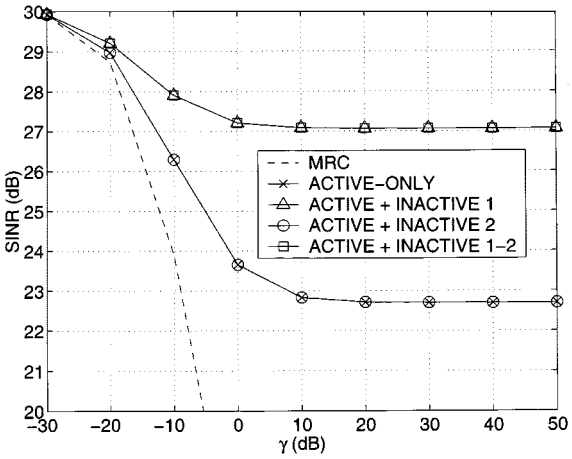

(b)

Fig. 6. Example 2. A seven-sensor eight-user uplink system. (a) Active and inactive coordinate sets. (b) SINR as a function of interference powers.

of kth user is $\rho_k = \|\mathbf{h}_k\|^2$ with $\rho_1 = 1$. The SNR of the desired user is 30 dB. We assume $\rho_2 = \rho_3 = \cdots = \rho_8 = \gamma$. Gold codes of length $M = 31$ are used signature waveforms. Chip-domain sampling is used, i.e., $B = 1/T_c$ in (3), where T_c denotes the chip duration. This corresponds to $M = 31$ samples per symbol. The SINRs of the MRC receiver and the LCMV multiuser receivers are compared for different number of inactive coordinates. In all the examples, the number of interfering users is fixed ($K - 1 = 7$) and the multipath delays and angles of arrival for the interfering users are given in Table I. The active coordinates of the desired user vary between different examples. A seven-element $\lambda/2$-spaced uniform linear array is simulated. The seven spatial basis angles are chosen to obtain a set of orthogonal spatial basis vectors, as discussed in Section II-B. The first example is depicted in Fig. 5. Note that `Inactive 1–2` in Fig. 5 is the union of `Inactive 1` and `2`, plus $(\tau_1, \phi_1) \in \{3T_c, 4T_c\} \times \sin^{-1}\{-2/7, 4/7\}$. Thus, $N_A = N_I^{(1)} = N_I^{(2)} = 4$, and $N_T = 16$ for `Active + Inactive 1–2`. In this example, $D = K - 1 = 7$. As evident from Fig. 5, the receiver is near–far resistant when $N_T \geq 8$, consistent with the results of Section IV.

Fig. 6 depicts a second example with a different set of $N_A = 5$ active coordinates for user 1. When only active coordinates are used, it can be shown that $D = 4 < \min(N_A, K-1) = 5$. The rank deficiency is due to the absence of MAI in the active CSTC corresponding to $\phi_1 = -\sin^{-1}(4/7)$. Hence, the five active coordinates are sufficient to provide near–far resistance. Also, note that inactive coordinates corresponding to $\phi_1 \in \sin^{-1}\{\pm 6/7\}$ do not affect the performance since they contain no MAI.

To demonstrate the effect of channel estimation errors on receiver performance, a single sensor ($R = 1$), eight-user system is simulated. The multipath delays for the interfering users are the same as in Table I. The desired user's multipath delays (active coordinates) are $\{0, T_c, 2T_c, 3T_c, 4T_c\}$. The inactive coordinates correspond to the delays $\{8T_c, 9T_c, \ldots, 15T_c\}$. In this case, $N_I = 8 > D$. Estimation error $\mathbf{e}$ is modeled

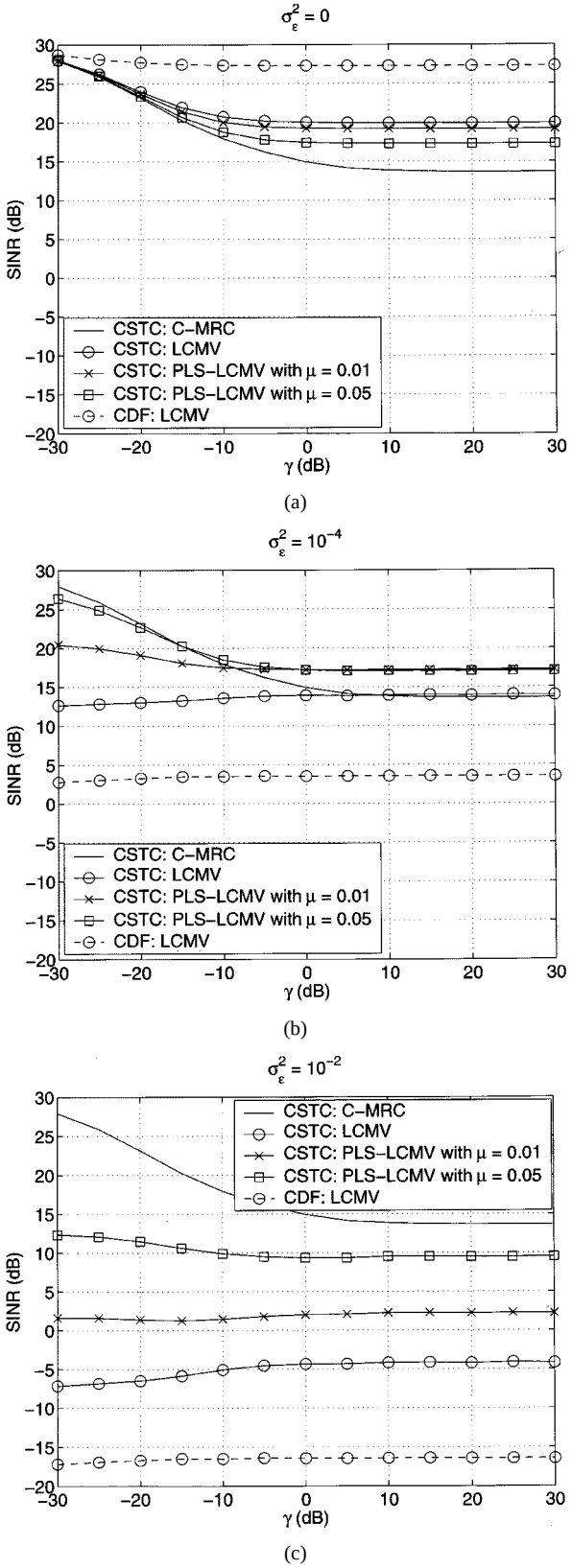

Fig. 7. Performance of different receivers in the presence of channel estimation error for 1-sensor system. For CSTC-based receivers, $N_A = 5$ and $N_I = 8$. (a) $\sigma_\varepsilon^2 = 0$. (b) $\sigma_\varepsilon^2 = 10^{-4}$. (c) $\sigma_\varepsilon^2 = 10^{-2}$.

as $\mathcal{N}_C[\mathbf{0}, \sigma_\varepsilon^2 \mathbf{I}_5]$. The estimation error variance is assumed unknown to the receiver. A serial structure receiver is used with $\mathbf{C} = \mathbf{R}_{AI}\mathbf{R}_{II}^{-1}$. We compare the performance of three different choices of $\mathbf{g}_A$ for different values of estimation error variance σ_ε^2: the LCMV solution in (30), C-MRC, and PLS-LCMV solution using the norm constraint with the penalty parameters $\mu = 0.01$ and 0.05. The results for the receiver (53) based on chip-domain filtering (CDF) also provided for comparison. The estimation error for $\mathbf{r}_1$ in (53) is modeled as $\mathcal{N}_C[\mathbf{0}, \sigma_\varepsilon^2 \mathbf{I}_{31}]$. Note that for a given number of samples and signal energy, the error variance per parameter for chip rate filtering should be larger than that for the CSTC-based receiver due to the larger number of parameters in the former. Thus, the use of same error variance σ_ε^2 provides an upper bound on the performance of chip-domain filtering schemes.

Fig. 7(a)–(c) depicts the SINR averaged over 2000 realizations of $\mathbf{e}$ for $\sigma_\varepsilon^2 = 0, 10^{-4}, 10^{-2}$. Observe that the CSTC-based LCMV solution is superior to other CSTC-based schemes when σ_ε^2 is small, yet inferior to others as σ_ε^2 increases. SINR degradation in LCMV and PLS-LCMV as σ_ε^2 increases is a result of desired signal cancellation due to channel estimation error. The SINR of the C-MRC approach is largely invariant to σ_ε^2 because it does not use $\hat{\mathbf{h}}_1$ for MAI suppression. It is clearly superior for relatively large σ_ε^2, but when σ_ε^2 is small, C-MRC inferior to LCMV and PLS-LCMV as it utilizes fewer dimensions to suppress MAI. In the absence of channel estimation error, the CDF LCMV receiver offers better performance because 30 degrees of freedom are available for MAI suppression. However, its performance degrades rapidly as the error variance increases. This increase in sensitivity to σ_ε^2 is due to the 31 channel parameters as opposed to only 5 channel parameters in the CSTC-based receiver.

IX. Conclusion

The CSTC framework introduced in [16] offers a natural platform for designing low-complexity multiuser receivers. The signal space partitioning into active coordinates containing the desired user's signal, and inactive coordinates containing only MAI provides a systematic approach to trade receiver complexity for MAI suppression capability. LCMV-based decentralized multiuser detectors are designed and analyzed. Extensions to general binary signaling with either coherent or noncoherent reception are also discussed. It is shown that the receiver is near–far resistant as long as the total number of active and inactive coordinates is greater than the effective rank of the MAI. A channel estimation technique that utilizes only inactive coordinates to suppress MAI is proposed. In the presence of channel estimation error, desired signal cancellation may occur. Two means are suggested to alleviate the resulting loss in performance. It is demonstrated that CSTC-based receivers promise superior performance compared to conventional chip-domain filtering schemes due to three main factors: reliable channel estimation, reliable data covariance matrix estimation, and robustness to channel estimation errors.

Appendix

Let $\mathbf{B}_A$ be the active coordinates basis matrix of size N_A. Let $\mathbf{B}_I^{(1)}$ be an inactive coordinate basis matrix of size $N_I^{(1)}$, and $\mathbf{B}_I^{(2)}$ be another such matrix of size $N_I^{(2)}$. Assume $[\mathbf{B}_A \ \ \mathbf{B}_I^{(1)} \ \ \mathbf{B}_I^{(2)}]$ is full column-rank and

$$\mathbf{\Omega}^{-1} = \begin{bmatrix} (\mathbf{\Omega}_{AA} - \mathbf{\Omega}_{AI}\mathbf{\Omega}_{II}^{-1}\mathbf{\Omega}_{AI}^{H})^{-1} & -\mathbf{\Omega}_{AA}^{-1}\mathbf{\Omega}_{AI}(\mathbf{\Omega}_{II} - \mathbf{\Omega}_{AI}^{H}\mathbf{\Omega}_{AA}^{-1}\mathbf{\Omega}_{AI})^{-1} \\ -(\mathbf{\Omega}_{II} - \mathbf{\Omega}_{AI}^{H}\mathbf{\Omega}_{AA}^{-1}\mathbf{\Omega}_{AI})^{-1}\mathbf{\Omega}_{AI}^{H}\mathbf{\Omega}_{AA}^{-1} & (\mathbf{\Omega}_{II} - \mathbf{\Omega}_{AI}^{H}\mathbf{\Omega}_{AA}^{-1}\mathbf{\Omega}_{AI})^{-1} \end{bmatrix} = \begin{bmatrix} \mathbf{W}_{11} & \mathbf{W}_{12} \\ \mathbf{W}_{12}^{H} & \mathbf{W}_{22} \end{bmatrix} \tag{55}$$

$N_A + N_I^{(1)} + N_I^{(2)} < RM$. Define $\mathrm{SINR}(\mathbf{X})$ to be the SINR obtained by using the coordinates induced by the basis matrix $\mathbf{X}$. We prove in this appendix that

$$\begin{aligned} \mathrm{SINR}(\mathbf{B}_A) &\le \mathrm{SINR}([\mathbf{B}_A \quad \mathbf{B}_I^{(1)}]) \\ &\le \mathrm{SINR}([\mathbf{B}_A \quad \mathbf{B}_I^{(1)} \quad \mathbf{B}_I^{(2)}]). \end{aligned} \tag{54}$$

We only prove the first inequality since the second inequality can be proved in a similar way. From (37), it suffices to show that $(\mathbf{\Gamma}_A^H\mathbf{\Omega}_{AA}^{-1}\mathbf{\Gamma}_A + \sigma^2\mathbf{I})^{-1} - (\mathbf{\Gamma}^H\mathbf{\Omega}^{-1}\mathbf{\Gamma} + \sigma^2\mathbf{I})^{-1}$ is nonnegative definite. Let $\mathbf{D} = \mathbf{\Gamma}_A^H\mathbf{\Omega}_{AA}^{-1}\mathbf{\Gamma}_A + \sigma^2\mathbf{I}$ and $\mathbf{M} = \mathbf{\Gamma}^H\mathbf{\Omega}^{-1}\mathbf{\Gamma} - \mathbf{\Gamma}_A^H\mathbf{\Omega}_{AA}^{-1}\mathbf{\Gamma}_A$. Then, it suffices to show that $\mathbf{D}^{-1} - (\mathbf{D}+\mathbf{M})^{-1} = \mathbf{D}^{-1}(\mathbf{D}^{-1} + \mathbf{M}^{-1})^{-1}\mathbf{D}^{-1}$ is nonnegative definite. Since $\mathbf{\Omega}_{AA}$ is positive definite, $\mathbf{D}$ and hence $\mathbf{D}^{-1}$ is positive definite. It follows from the definition of positive definiteness that for any full column-rank matrix $\mathbf{X}$, $\mathbf{X}^H\mathbf{P}\mathbf{X}$ is positive definite if $\mathbf{P}$ is positive definite. To show that $\mathbf{M}$ is nonnegative definite, we define (55), shown at the top of the page. Applying (55) and (16), we have

$$\begin{aligned} \mathbf{M} &= \mathbf{\Gamma}_A^H(\mathbf{W}_{11} - \mathbf{\Omega}_{AA}^{-1})\mathbf{\Gamma}_A + \mathbf{\Gamma}_A^H\mathbf{W}_{12}\mathbf{\Gamma}_I \\ &\quad + \mathbf{\Gamma}_I^H\mathbf{W}_{12}^H\mathbf{\Gamma}_A + \mathbf{\Gamma}_I^H\mathbf{W}_{22}\mathbf{\Gamma}_I, \\ \mathbf{W}_{11} - \mathbf{\Omega}_{AA}^{-1} &= \mathbf{\Omega}_{AA}^{-1}\mathbf{\Omega}_{AI}\mathbf{W}_{22}\mathbf{\Omega}_{AI}^H\mathbf{\Omega}_{AA}^{-1}. \end{aligned} \tag{56}$$

Notice that $\mathbf{W}_{22}^{-1}$ is the Schur-complement of $\mathbf{\Omega}$, hence it is nonnegative definite [22], and so is $\mathbf{W}_{22}$. Cholesky factoring $\mathbf{W}_{22} = \mathbf{S}\mathbf{S}^H$ and defining $\mathbf{U} = \mathbf{\Omega}_{AI}^H\mathbf{\Omega}_{AA}^{-1}$, we have $\mathbf{W}_{11} - \mathbf{\Omega}_{AA}^{-1} = \mathbf{U}^H\mathbf{S}\mathbf{S}^H\mathbf{U}$, $\mathbf{W}_{12} = -\mathbf{U}^H\mathbf{S}\mathbf{S}^H$, and $\mathbf{W}_{22} = \mathbf{S}\mathbf{S}^H$. Hence

$$\mathbf{M} = (\mathbf{U}\mathbf{\Gamma}_A - \mathbf{\Gamma}_I)^H\mathbf{S}\mathbf{S}^H(\mathbf{U}\mathbf{\Gamma}_A - \mathbf{\Gamma}_I) \tag{57}$$

which implies that $\mathbf{M}$ is nonnegative definite, and so is $\mathbf{M}^{-1}$. Thus, $(\mathbf{D}^{-1} + \mathbf{M}^{-1})^{-1}$ is *positive definite*. Hence, we have proved the first inequality. □

REFERENCES

[1] U. Madhow and M. L. Honig, "MMSE interference suppression for direct-sequence spread-spectrum CDMA," *IEEE Trans. Commun.*, vol. 42, pp. 3178–3188, Dec. 1994.

[2] M. L. Honig, U. Madhow, and S. Verdu, "Blind adaptive multiuser detection," *IEEE Trans. Inform. Theory*, vol. IT-41, pp. 944–960, July 1995.

[3] X. Wang and H. V. Poor, "Blind multiuser detection: A subspace approach," *IEEE Trans. Inform. Theory*, vol. 44, pp. 677–690, Mar. 1998.

[4] U. Madhow, "Blind adaptive interference suppression for direct-sequence CDMA," *Proc. IEEE*, vol. 86, pp. 2049–2069, Oct. 1998.

[5] X. Wang and H. V. Poor, "Space–time multiuser detection in multipath CDMA channels," *IEEE Trans. Signal Processing*, vol. 47, pp. 2356–2374, Sept. 1999.

[6] M. K. Tsatsanis and Z. Xu, "Performance analysis of minimum variance CDMA receivers," *IEEE Trans. Signal Processing*, vol. 46, pp. 3014–3022, Nov. 1998.

[7] I. Ghauri and D. T. Slock, "Blind channel and linear MMSE receiver determination in DS-CDMA systems," in *Proc. 1999 ICASSP*, 1999.

[8] M. L. Honig and J. S. Goldstein, "Adaptive reduced-rank interference suppression based on the multistage wiener filter," *IEEETrans. Commun.*, submitted for publication.

[9] S. Y. Miller and S. C. Schwartz, "Integrated spatial–temporal detectors for asynchronous Gaussian multiple-access channels," *IEEE Trans. Commun.*, vol. 43, pp. 396–411, Feb./Mar./Apr. 1995.

[10] R. Kohno, "Spatial and temporal filtering for co-channel interference in cdma," in *IEEE 1994 Spread Spectrum Techniques and Applications (ISSSTA 1994)*, pp. 51–60.

[11] A. J. Paulraj and C. B. Papadias, "Space–time processing for wireless communications," *IEEE Signal Processing Mag.*, pp. 49–83, Nov. 1997.

[12] X. Bernstein and A. M. Haimovich, "Space–time optimum combining for cdma communications," *Wireless Pers. Commun.*, 1996.

[13] A. Yener, R. D. Yates, and S. Ulukus, "Interference management for cdma systems through power control, multiuser detection, and beamforming," *IEEE Trans. Commun.*, vol. 49, pp. 1227–1239, July 2001.

[14] ——, "Joint power control, multiuser detection and beamforming for cdma systems," in *IEEE 49th Vehicular Technology Conf., VTC 1999*, pp. 1032–1036.

[15] ——, "Combined temporal and spatial filter structures for cdma systems," in *IEEE 52nd Vehicular Technology Conf., VTC Fall 2000*, pp. 2386–2393.

[16] E. N. Onggosanusi, A. M. Sayeed, and B. D. Van Veen, "Canonical space–time processing for wireless communications," *IEEE Trans. Commun.*, vol. 48, pp. 1669–1680, Oct. 2000.

[17] ——, "Low complexity space–time multiuser detectors," in *Proc. 1999 IEEE Wireless Commun. and Network Conf. WCNC*.

[18] S. Haykin, *Adaptive Filter Theory*, 3rd ed. Englewood Clifs, NJ: Prentice-Hall, 1996.

[19] T. F. Wong, T. M. Lok, J. S. Lehnert, and M. D. Zoltowski, "A linear receiver for direct-sequence spread-spectrum multiple-access systems with antenna arrays and blind adaptation," *IEEE Trans. Inform. Theory*, vol. 44, pp. 659–676, Mar. 1998.

[20] J. Ramos, M. D. Zoltowski, and H. Liu, "Low-complexity space–time processor for DS-CDMA communications," *IEEE Trans. Signal Processing*, vol. 48, pp. 39–52, Jan. 2000.

[21] J. Brewer, "Kronecker products and matrix calculus in system theory," *IEEE Trans. Circuits Syst.*, vol. CAS-25, pp. 772–781, Sept. 1978.

[22] L. L. Scharf, *Statistical Signal Processing*. Reading, MA: Addison-Wesley, 1991.

[23] S. Verdu, *Multiuser Detection*. Cambridge, U.K.: Cambridge Univ. Press, 1998.

[24] B. D. Van Veen, A. M. Sayeed, and E. N. Onggosanusi, "Interference resistant blind acquisition and channel estimation for CDMA communication systems," in *Proc. ICASSP 2000*, vol. 5, Istanbul, Turkey, pp. 2913–2416.

[25] T. A. Kadous and A. M. Sayeed, "Decentralized multiuser detection for time-varying multipath channels," *IEEE Trans. Commun.*, vol. 48, pp. 1840–1852, Nov. 2000.

[26] B. D. Van Veen, "Minimum variance beamforming with soft response constraints," *IEEE Trans. Signal Processing*, vol. 39, pp. 1964–1972, Sept. 1991.

[27] H. Cox, R. M. Zeskind, and M. M. Owen, "Robust adaptive beamforming," *IEEE Trans. Acoust., Speech, Signal Processing*, vol. ASSP-35, pp. 1365–1376, Oct. 1987.

[28] . [Online]. Available: http://www.3gpp.org

[29] B. D. Van Veen, "Adaptive convergence of linearly constrained beamformers based on the sample covariance matrix," *IEEE Trans. Signal Processing*, vol. 39, pp. 1470–1473, June 1991.

Eko N. Onggosanusi (M'01) received the B.Sc. (with highest distinction), M.Sc., and Ph.D. degrees from the University of Wisconsin-Madison, all in electrical and computer engineering, in 1996, 1998, and 2000, respectively.

During the summer of 1999 and 2000, he was a visiting student at the DSPS R&D Texas Instruments, Dallas, TX, working on antenna array diversity for wideband CDMA and adaptive modulation and coding for wireless personal area networks, respectively. Since January 2001, he has been with the DSPS R&D Texas Instruments, where he is currently a member of technical staff in the Mobile Wireless Branch of Communication Systems Laboratory. He is currently working on the third-generation wireless communication systems, focusing on high-data-rate techniques and applications. His research interests include signal processing, information theory, and channel coding for digital communications.

Akbar M. Sayeed (S'87–M'97) received the B.S. degree from the University of Wisconsin-Madison in 1991 and the M.S. and Ph.D. degrees from the University of Illinois at Urbana-Champaign in 1993 and 1996, respectively, both in electrical and computer engineering.

While at the University of Illinois, he was a Research Assistant in the Coordinate Science Laboratory and was also the Schlumberger Fellow in signal processing from 1992 to 1995. During 1996–1997, he was a Post-Doctoral Fellow at Rice University, Houston, TX. Since August 1997, he has been with the University of Wisconsin-Madison, where he is currently an Assistant Professor in Electrical and Computer Engineering. His research interests are in wireless communications, statistical signal processing, time-frequency and wavelet analysis.

Dr. Sayeed received the NSF CAREER Award in 1999 and the ONR Young Investigator Award in 2001. He is currently serving as an Associate Editor for IEEE SIGNAL PROCESSING LETTERS.

Barry D. Van Veen (S'81–M'86–SM'97–F'02) was born in Green Bay, WI. He received the B.S. degree from Michigan Technological University in 1983 and the Ph.D. degree from the University of Colorado in 1986, both in electrical engineering. He was an ONR Fellow while working on the Ph.D. degree.

In the spring of 1987, he was with the Department of Electrical and Computer Engineering at the University of Colorado-Boulder. Since August of 1987, he has been with the Department of Electrical and Computer Engineering at the University of Wisconsin-Madison and currently holds the rank of Professor. His research interests include signal processing for sensor arrays, nonlinear systems, adaptive filtering, wireless communications and biomedical applications of signal processing. He co-authored *Signals and Systems* (New York: Wiley, 1999) with Simon Haykin.

Dr. Van Veen was a recipient of a 1989 Presidential Young Investigator Award from the National Science Foundation and a 1990 IEEE Signal Processing Society Paper Award. He served as an Associate Editor for the IEEE TRANSACTIONS ON SIGNAL PROCESSING and Signal Processing and on the IEEE Signal Processing Society's Technical Committee on Statistical Signal and Array Processing from 1991 through 1997 and is currently a member of the Sensor Array and Multichannel Technical Committee. He received the Holdridge Teaching Excellence Award from the Electrical and Computer Engineering Department at the University of Wisconsin in 1997.